UNIVERSITY of York

This is a repository copy of *Development of 3D graph-based model to examine photovoltaic micro cracks*.

White Rose Research Online URL for this paper:
https://eprints.whiterose.ac.uk/id/eprint/177694/

Version: Accepted Version

Article:
Dhimish, Mahmoud, Holmes, Violeta, Mather, Peter et al. (2 more authors) (2018) Development of 3D graph-based model to examine photovoltaic micro cracks. Journal of Science: Advanced Materials and Devices. pp. 380-388. ISSN: 2468-2284

https://doi.org/10.1016/j.jsamd.2018.07.004

Reuse
Items deposited in White Rose Research Online are protected by copyright, with all rights reserved unless indicated otherwise. They may be downloaded and/or printed for private study, or other acts as permitted by national copyright laws. The publisher or other rights holders may allow further reproduction and re-use of the full text version. This is indicated by the licence information on the White Rose Research Online record for the item.

Takedown
If you consider content in White Rose Research Online to be in breach of UK law, please notify us by emailing eprints@whiterose.ac.uk including the URL of the record and the reason for the withdrawal request.

White Rose university consortium
Universities of Leeds, Sheffield & York

eprints@whiterose.ac.uk
https://eprints.whiterose.ac.uk/

Development of 3D Graph-Based Model to Examine Photovoltaic Micro Cracks

Abstract*:* This paper presents a novel technique to examine the impact of Photovoltaic (PV) micro cracks on the performance of the output power for PV solar cells. Initially, the image of the PV micro crack is captured using Electroluminescence (EL) method, then processed by the proposed technique. The technique consist of two stages, the first stage combines two images using an OR gate, the first image is the crack-free (healthy) solar cell, whereas the second is the cracked solar cell image. The output image from the first stage is passed into the second stage which uses a 3D graph-based model in order to examine the output power loss in the cracked solar cell. In order to examine the effectiveness of the 3D graph-based model, two different cracked PV solar cells have been examined. From the obtained results, it was evident that the micro cracks size, location, and orientation more detectible using the developed technique. In addition, the maximum and minimum output power also can be estimated using the offered technique.

Keywords: Photovoltaic; Solar Cells; Micro Cracks Detection; Electroluminescence (EL); Power Loss.

---

1. Introduction

Micro cracks in solar cells are a genuine problem for Photovoltaic (PV) modules. They are hard to avoid and, up to date, the impact of PV micro cracks on the performance of the PV modules in various environmental conditions has not been reported [1 - 3]. In order to examine micro cracks in PV modules, several methods have been proposed [4]. Resonance ultrasonic vibrations (RUV) technique for crack detection in PV silicon wafers has been developed by [5 and 6].

RUV technique uses ultrasonic vibrations of a tenable frequency and changeable amplitude. The silicon wafer is constrained by an external piezoelectric transducer in a frequency range of 20 to 90 kHz. The transducer comprises a central hole allowing a reliable vacuum coupling between the wafer and transducer by applying 50-kPa negative pressure to the backside of the wafer. RUV PV micro crack technique is sensitive to crack length and its location, and can be used to reject or accept wafers. However, it does not identify the precise location of the PV crack.

Photoluminescence (PL) aiming technique was proposed to solve this problem, since it can be used to inspect micro cracks in silicon wafers and PV modules [7]. PL technique can be applied not only at the end of the PV solar cell's production, but also it can be slotted in during the process of production [8].

Y. Zhu et al. [9] proposed a new PL setup that enables inhomogeneous illumination with arbitrary illumination patterns to determine various parameters of solar cells. The results indicate that the use of inhomogeneous illumination significantly extends the range of photoluminescence imaging applications for the characterization of silicon wafers and solar cells.

Most recently, in 2018, the PL images are acquired using the sun as the sole illumination source by separating the weak luminescence signal from the much stronger ambient sunlight signal. This is done by using a suitable optical filtering and modulation of the PV cells biasing between the normal operating point and open circuit conditions [10].

Electroluminescence (EL) technique is another method for the micro crack detection in PV solar cells. EL technique is the form of luminescence in which electrons are excited into the conduction band through the use of electrical current by connecting the solar cell in forward bias mode. This technique is very attractive, because it can be used not only with small solar cell sizes but also, it can be used with full scale PV modules [11 and 12].

The EL method requires the solar cells to be in the forward bias condition in order to emit infrared radiation. The EL ranges from 950 to 1250 nm with the peak occurring at approximately 1150 nm. Emission intensity is dependent on the density of defects in the silicon, with fewer defects resulting in more emitted photons [13]. The EL system should be placed in a dark room, as the image of the cells is being taken by cooled CCD camera, we have already published the configuration and construction of the EL setup in [14].

M. Kontgers et al. [15], investigated the impact of micro cracks on the performance of PV modules using EL imaging method. This research proves that micro cracks do not reduce the power generation of a PV module by more than 2.5%, if the crack does not harm the electrical contact between the cell and fragments. Orientational distribution of micro cracks in crystalline PV cells was firstly presented by S. Kajari-Schröder et al. [16]. PV micro cracks were classified into six sub categories as follows: dendritic, several, +450, -450, Parallel to busbars, and Perpendicular to busbars.

The analysis have been carried out using 27 PV modules using EL imaging technique, where the maximum micro cracks found in the PV modules is parallel to busbars with 50% relative occurrence. Furthermore, I-V curve analysis based on gallium arsenide (GaAs) PV solar cell on silicon substrate for crack-free and cracked PV solar cells have been investigated by S. Oh et al. [17] using EL imaging technique. It was evident that the output voltage of the PV solar cells decrease while increasing the crack size. Moreover, the crack density defined as the total length of the crack liner per unit area, which was found to be in the range from 13.8 to 33.2 cm-1 in most investigated solar cell samples.

On the other hand, in 2018 a new micro crack detection method based on self-learning features and low-rank matrix recovery was proposed by X. Qian et al. [18]. Firstly, the input image is pre-processed to suppress the noises and remove the busbars and fingers. Next, a self-learning feature extraction scheme in

which the feature extraction patterns are changed along with the input image is introduced. Finally, the optimized result is further fine-tuned by morphological post processing.

In this paper, EL imaging technique was used to capture the micro cracks in PV solar cells. The EL detection technique is already shown in our previous articles [11 and 19]. Furthermore, the main contribution is illustrated as follows:

- Technique selection: comparing different techniques to assess crack-free and cracked solar cell output EL image
- Image resolution: selecting the most suitable technique that has an optimum observable output image arrangement, in which it can be used to precisely identify PV crack orientation, size, and location
- Surface analysis: process the desirable image into a suitable system in order to draw a relevant graph-based description for the power loss in the cracked PV solar cell

This paper is organized as follows: **Section 2** explains the examined PV module and its electrical specifications. **Section 3** and **4** demonstrate various techniques for analyzing the PV crack images and the obtained results, while **Section 5** draws a relevant conclusion for the proposed power loss estimation of the cracked PV solar cells.

2. Tested PV Solar Cells

In this work, the tested PV modules are shown in Fig. 1(a), the total inspected PV modules are ten, where its maximum peak power is 220W and the number of solar cells is 60 per PV module.

A healthy (crack-free) solar cell is shown in Fig. 1(b), whereas a cracked solar cell is shown in Fig. 1(c). Both crack-free and cracked solar cell images will be processed using various detection techniques, this will be explained in the next section.

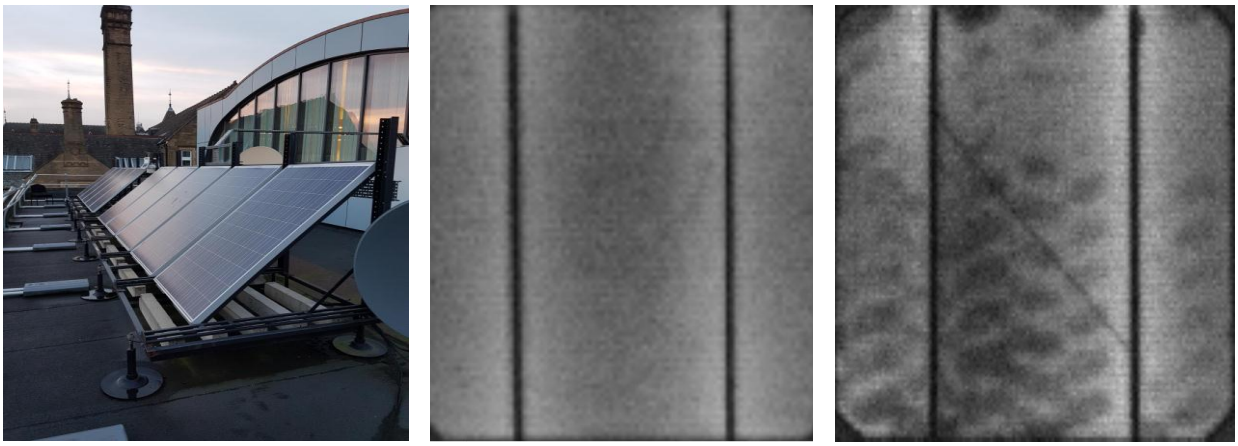

(a) (b) (c)

Fig. 1. (a) 10 Examined PV modules, (b) Healthy (crack-free) PV solar cell, (c) Cracked PV solar cell

3. Proposed Detection Technique

This section describes the selection for the proposed EL detection technique. Fig. 2 shows the combination between the healthy and cracked PV solar cells. Six different techniques were used to combine both images, staring with OR gate, ending with subtraction technique. The output image for each technique is also demonstrated in Fig. 2.

As can be noticed, the division technique has no output (fully black PV solar cell image), whereas the second worst output image when subtracting the healthy from the cracked image. However, the best image resolution for the crack is identified using the OR gate (healthy solar cell image OR cracked solar cell image), this result arises because the crack-free image would not add additional noise or cracks to the cracked solar cell image, however, it cleans up the areas which have no micro cracks.

Fig. 3(a) show the output image of the OR gate. As can be noticed, the image lacks filtering for the noise in the areas that have no micro cracks, thus, it is required to create an image with a better resolution. It is worthy pointing that both vertical line correspond to the solar cell busbars.

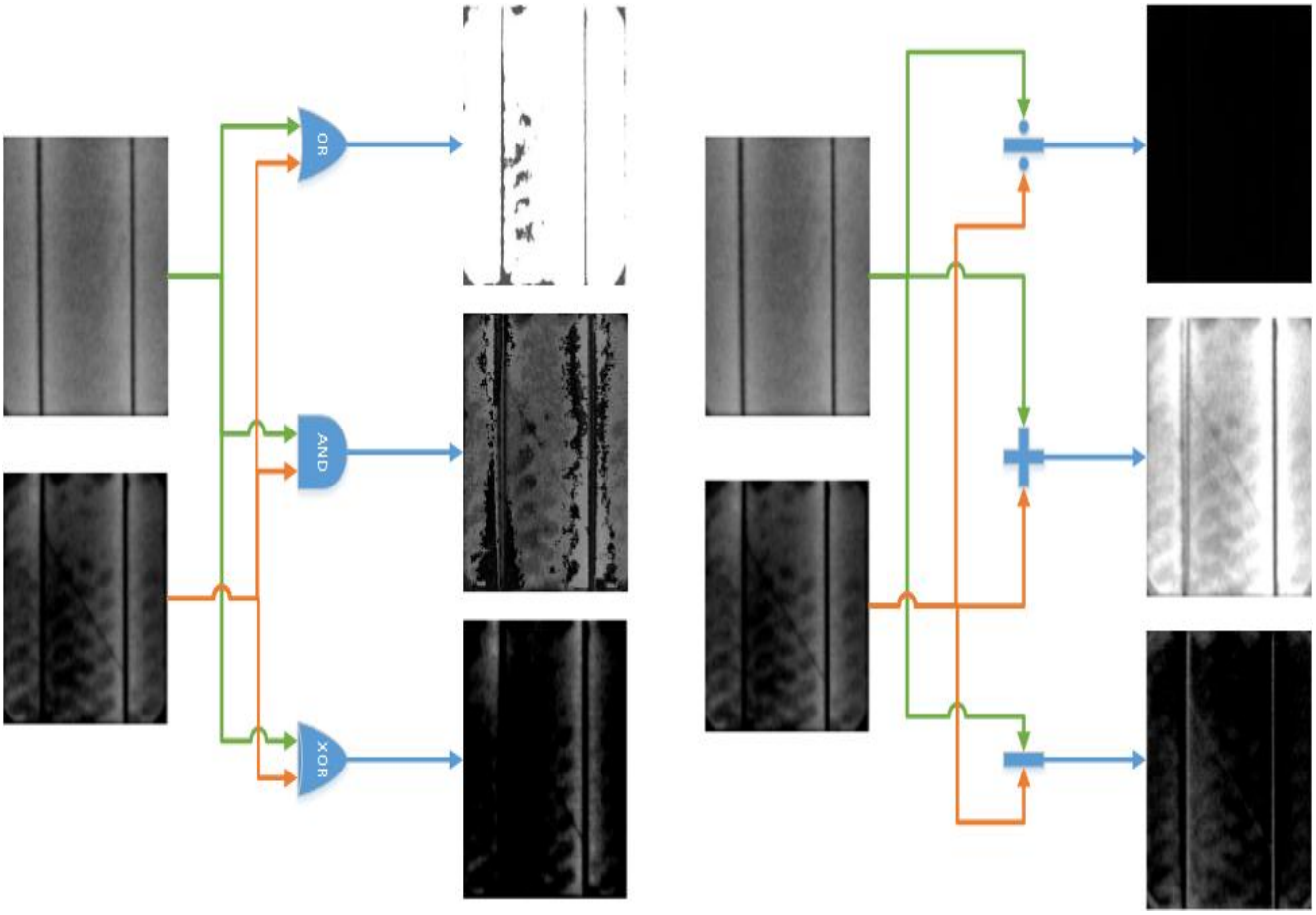

Fig. 2. The image of the healthy cell combined with cracked solar cell using various techniques (OR, AND, XOR, Division, Addition, Subtraction)

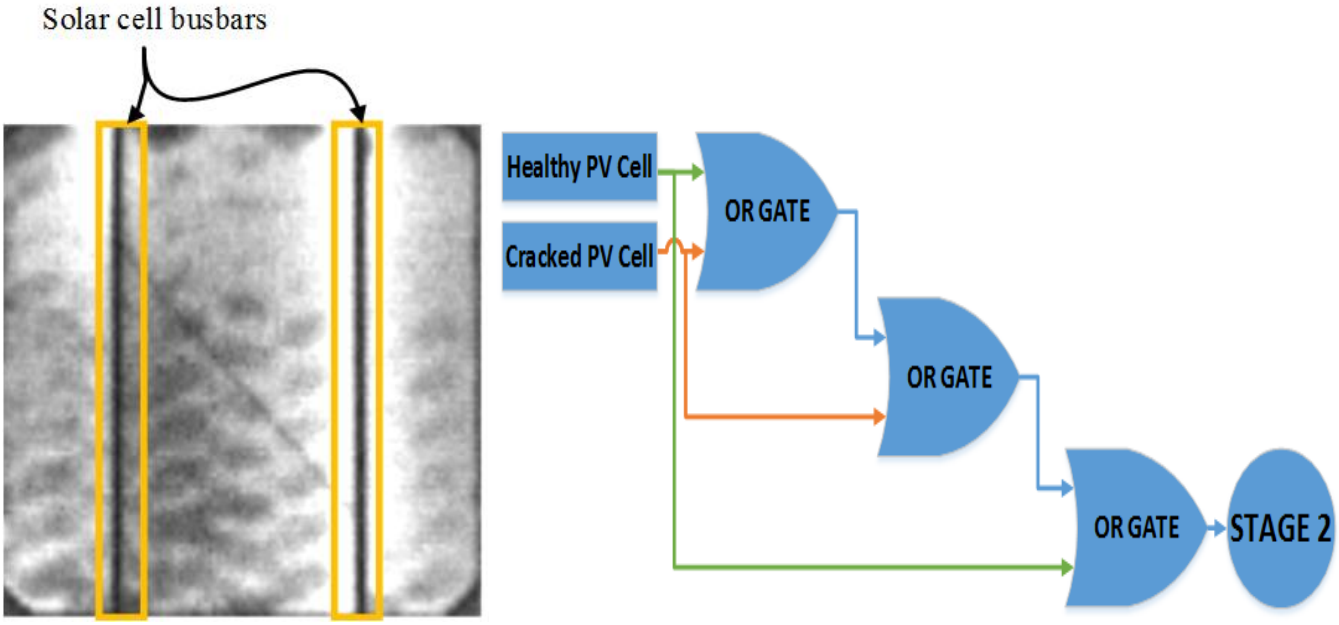

Fig. 3. (a) OR gate output result, (b) suggested image filtering and resolution enhancement technique

The proposed filtering and resolution enhancement technique is shown in Fig. 3(b). The suggested technique consists of three steps, each step has an OR gate. The healthy PV cell image plays a significant role in the correction of the whole output image, since it affects the first stage output result. The second and third OR gates filter the noise in the combined image of crack-free and cracked solar cell.

The Main functionality for each OR gate is presented in Fig. 4(a). In fact, each of the above listed techniques are based on a specific process which it will calibrate bit-by-bit of the pixels for the images, thus to clear out the noise, and improve the quality of the output cracked solar cell image, the process for 2 bits is described in Fig. 4(a). As a result, the detection technique leads for better image structure.

Fig. 4 shows the output images from each step using the proposed filtering and resolution enhancement technique. Fig. 4(b) shows the output images from all OR gates for stage 1.

It is evident that after the 3rd OR gate, the micro cracks do appear more visible in the size, location, and orientation compared to the original image shown previously in Fig. 1(c).

The maximum pixel resolution for all images is obtained by the third OR gate. In order to visualize this image in better conditions, another layer is added which basically calibrate the image form black-white into a color (i.e. cyan-green as shown in Fig. 4(c)). The selection of the color does not make significant difference in the output image resolution, since it does not add any noise, or interference with the resulted image.

The final calibrated image is passed to the second stage (Stage 2) shown previously in Fig. 3(b). The main purpose of this stage is to route the image into a 3D graph-based model in which it will outline the total output power loss in the cracked solar cell. This stage will briefly be described in the next section.

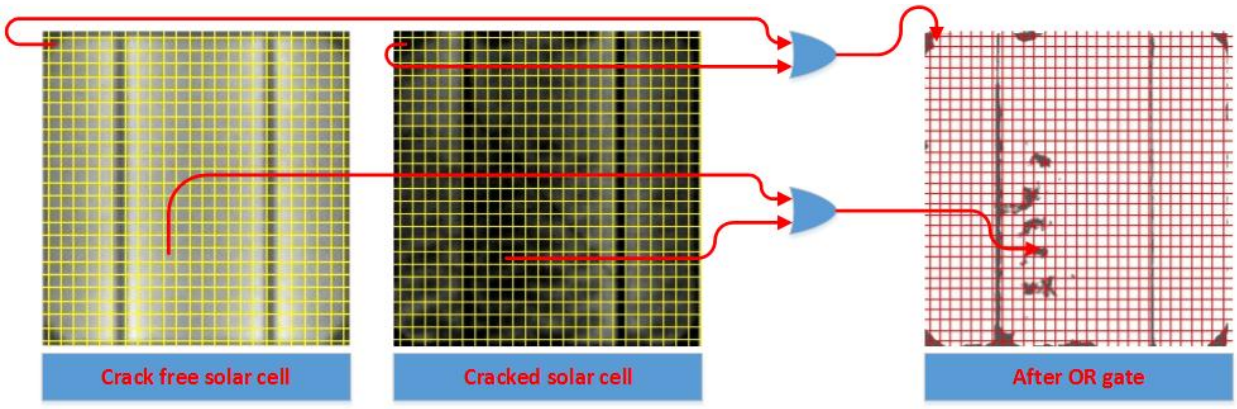

(a)

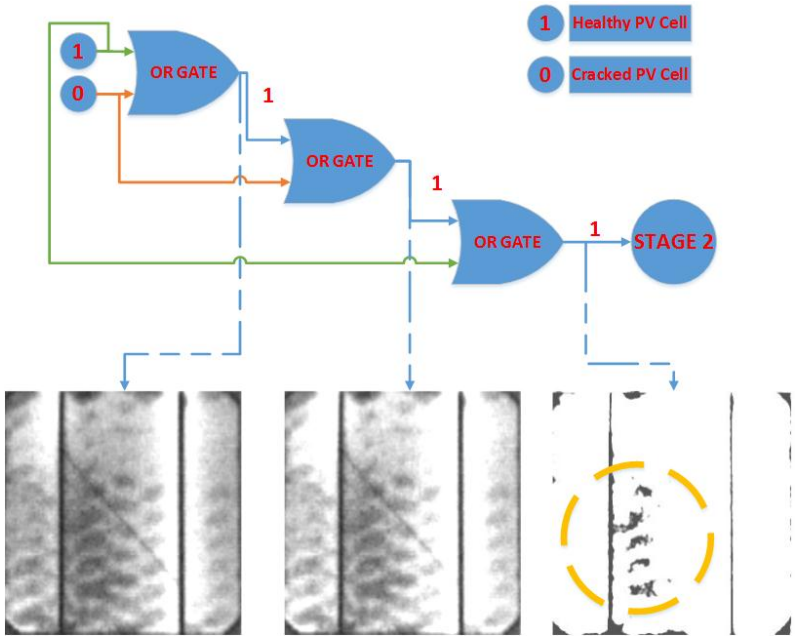

(b)

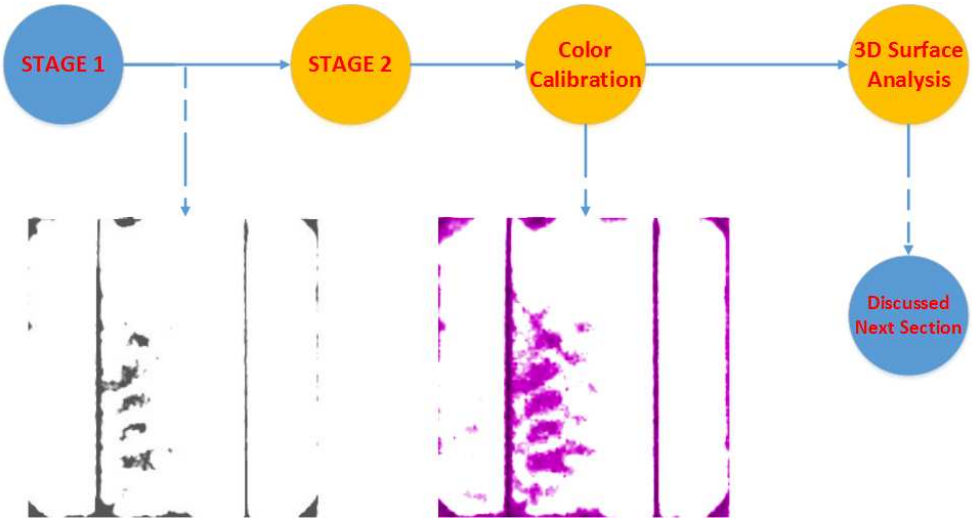

(c)

Fig. 4. (a) bit-by-bit pixel calibration after each OR gate, (b) Output PV solar cell image obtained by each OR gate, (c) Stage 2 color calibrated image

To sum up, the proposed micro crack detection techniques has a better resolution and focus for the micro crack size, location, and orientation. So, to end up this section, it would be sufficient to show the final black-and-white calibrated image vs. the original EL image captured by the camera.

Fig. 5 illustrates that before using the detection system, several cracks appears on the original EL image such as the micro cracks labelled “1” and “2”. Whereas after using the proposed technique it was evident that these are not actual cracks but a noise caused by the original EL image. In addition, the actual micro cracks size, location, and orientation are labelled as “3” on Fig. 5. These micro cracks in the solar cell are clearly detected and observed as shown in the figure.

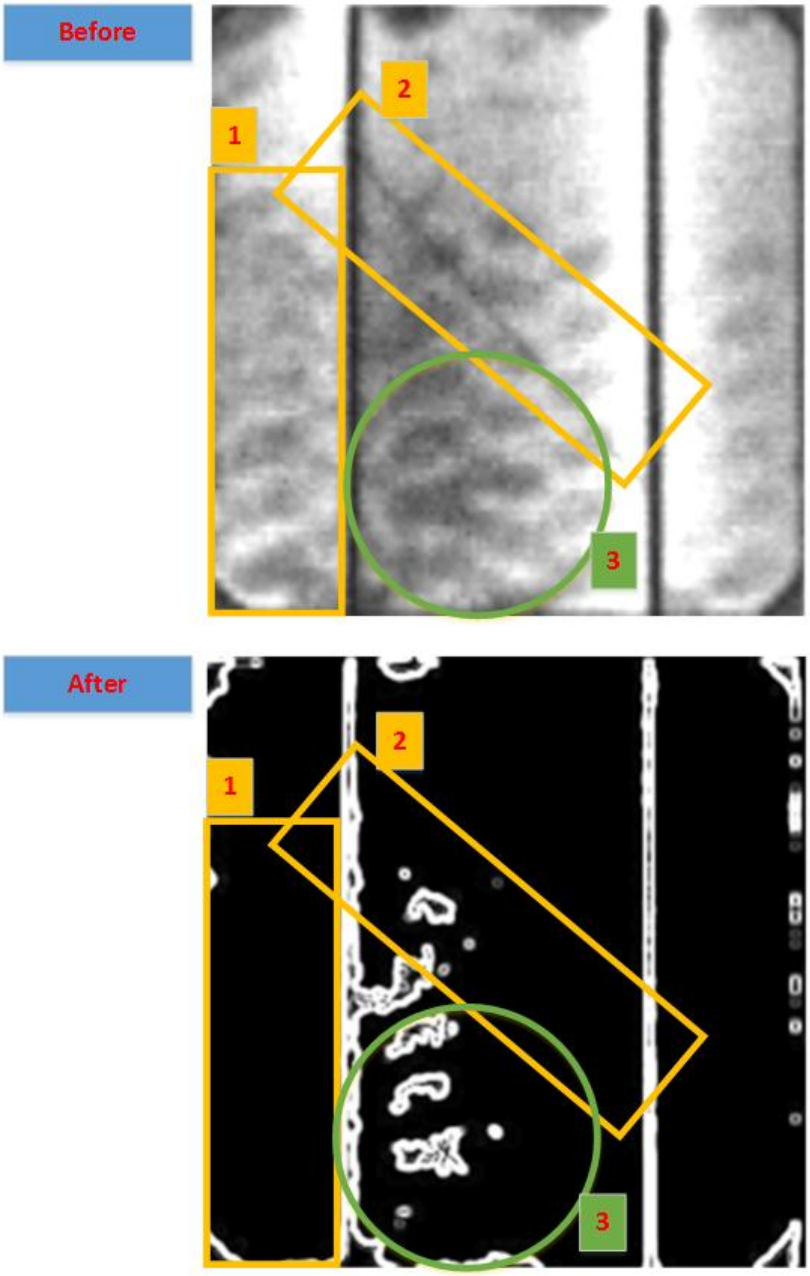

Fig. 5. Micro crack detection before and after the proposed technique

4. Graph-Based Model

4.1 Overall Structure and 3D Surface Implementation

The final image from the implemented filtering and resolution enhancement technique will be processed into a 3D graph-based model, the output of the model is shown in Fig. 6(a). In addition, Fig. 6(b) shows the 3D adjusted surface of the cracked PV solar cell, where x-axis and y-axis presents the pixel number of the calibrated image, and z-axis presents the output power of the solar cell. The 3D model is implemented using the image processing toolbox available in MATLAB [20].

The 3D graph-based model follows the following steps:

- Color calibration of the processed image from the last stage (filtering and resolution enhancement stage)
- Adjusting the pixel number and generating x-axis and y-axis
- Identifying the maximum output power of the solar cell, which is calculated using (1). Therefore, producing the z-axis of the 3D graph-based model

$$PV\ Cell\ Maximum\ Output\ Power\ = \frac{PV\ module\ peak\ power}{Number\ of\ PV\ solar\ cells\ in\ the\ PV\ module}$$

$$= \frac{220\ W}{60} = 3.6\ W \quad (1)$$

Therefore, it is possible to predict/calculated the output power loss due to the micro cracks based on the cumulative power shown as z-axis.

As shown in the 3D graph-based model, areas with free-cracks (healthy areas) generate a peak output power of 2.3 W, however, the cracked area does not produce any output power. Fig. 6(a) presents area "labelled with a circle" that has no micro cracks, and according to the 3D surface this area of the solar cell generates a peak power equals to the following:

$$Peak\ power = 230 \times 10^{-2} = 2.3W$$

Furthermore, there are various areas in the solar cell contain less output power (nearly 180 x 10^{-2} = 1.8W) from the initial construction of the 3D surface, hence, these areas comprise minor or major cracks. To sum up, the total maximum loss in the output power is calculated as follows:

Healthy PV cell peak power (2.3W) – Crack PV cell peak power (1.8W) = 0.5W.

Fig. 6(b) shows the adjusted/biased image from the initial processed image in the 3D graph-based model. This image shows that while simulating the PV under various illumination levels, the cracked areas of the solar cell generates less output power compared to healthy areas.

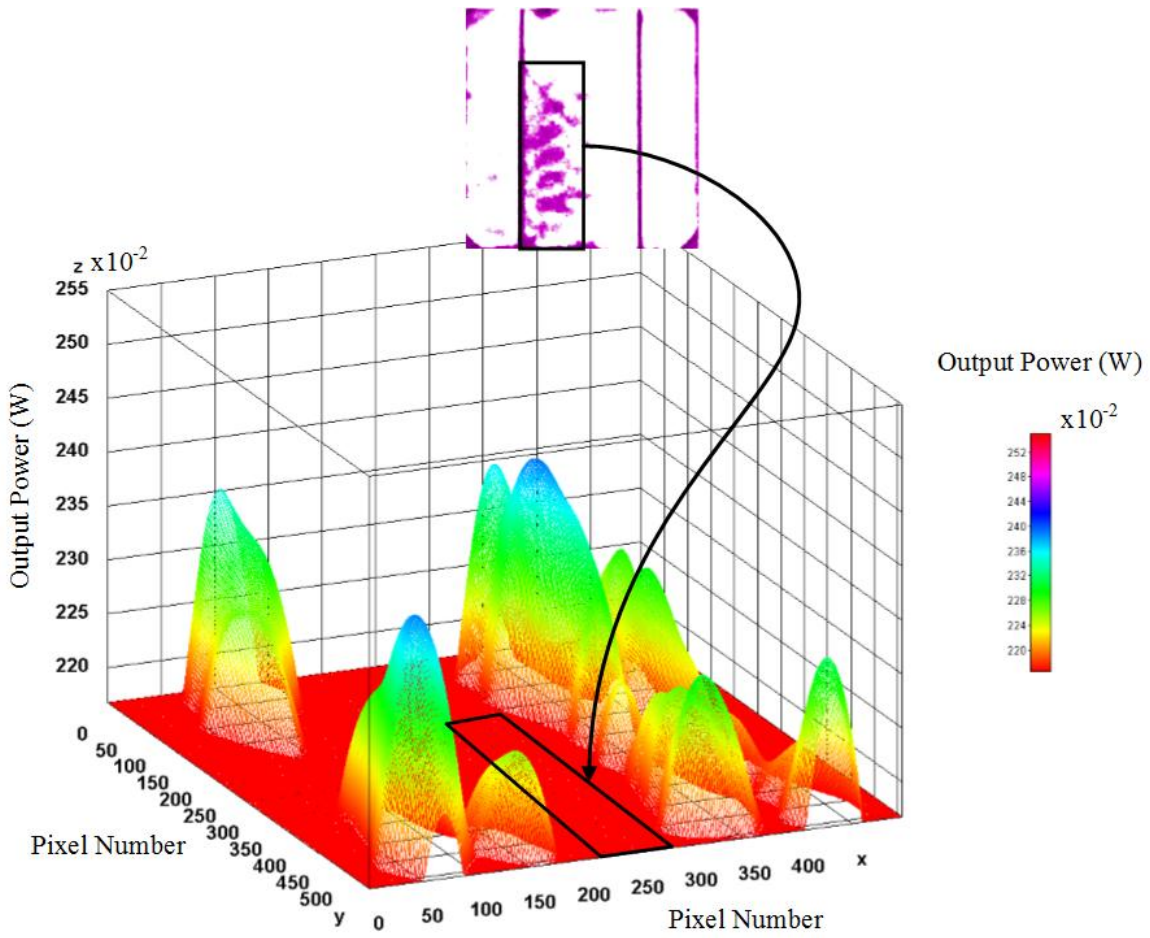

(a)

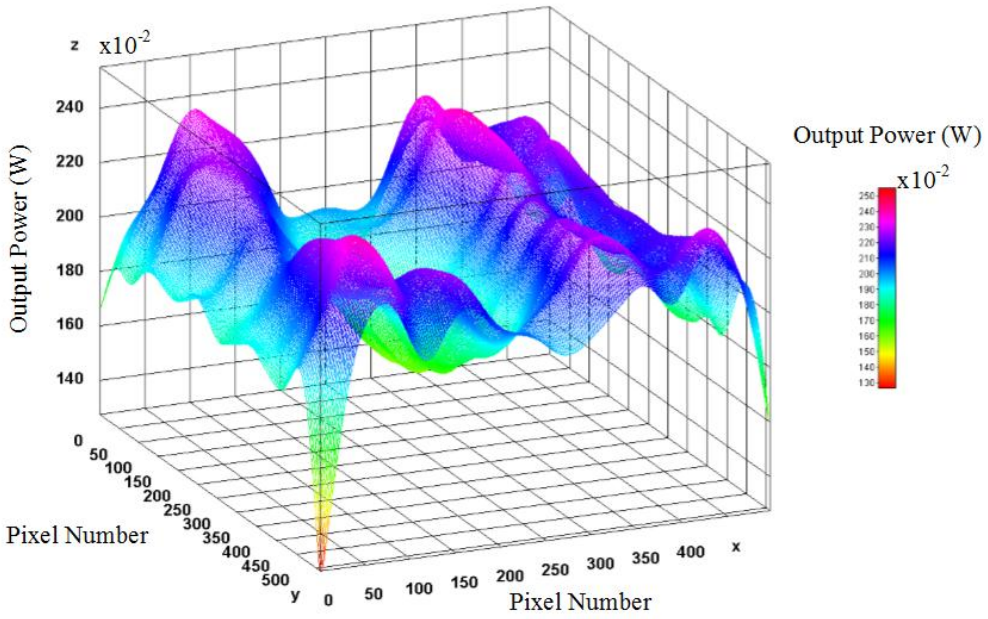

(b)

Fig. 6. (a) Initial 3D surface generated using the calibrated image of the cracked solar cell, (b) Adjusting the scale of the 3D image obtained in Fig. 5(a)

4.2 Evaluation of the Developed 3D Graph-Based Model

In order to test the effectiveness of the proposed 3D graph-based model for estimating the power loss of cracked PV cells, another PV cracked solar cell sample has been examined.

The examined healthy and cracked PV cell is shown in Fig. 7(a) and 7(b) respectively. The output of the first OR gate between the healthy and cracked is presented in Fig. 7(c). For better resolution, this image will be processed through two different OR gates, while the resulted images are shown in Fig. 7(d) and 7(e) respectively. As can be seen from the 3rd OR gate image, the crack location, size, and orientation is more clear, and it is much observable in terms of the areas that are affected by the micro cracks.

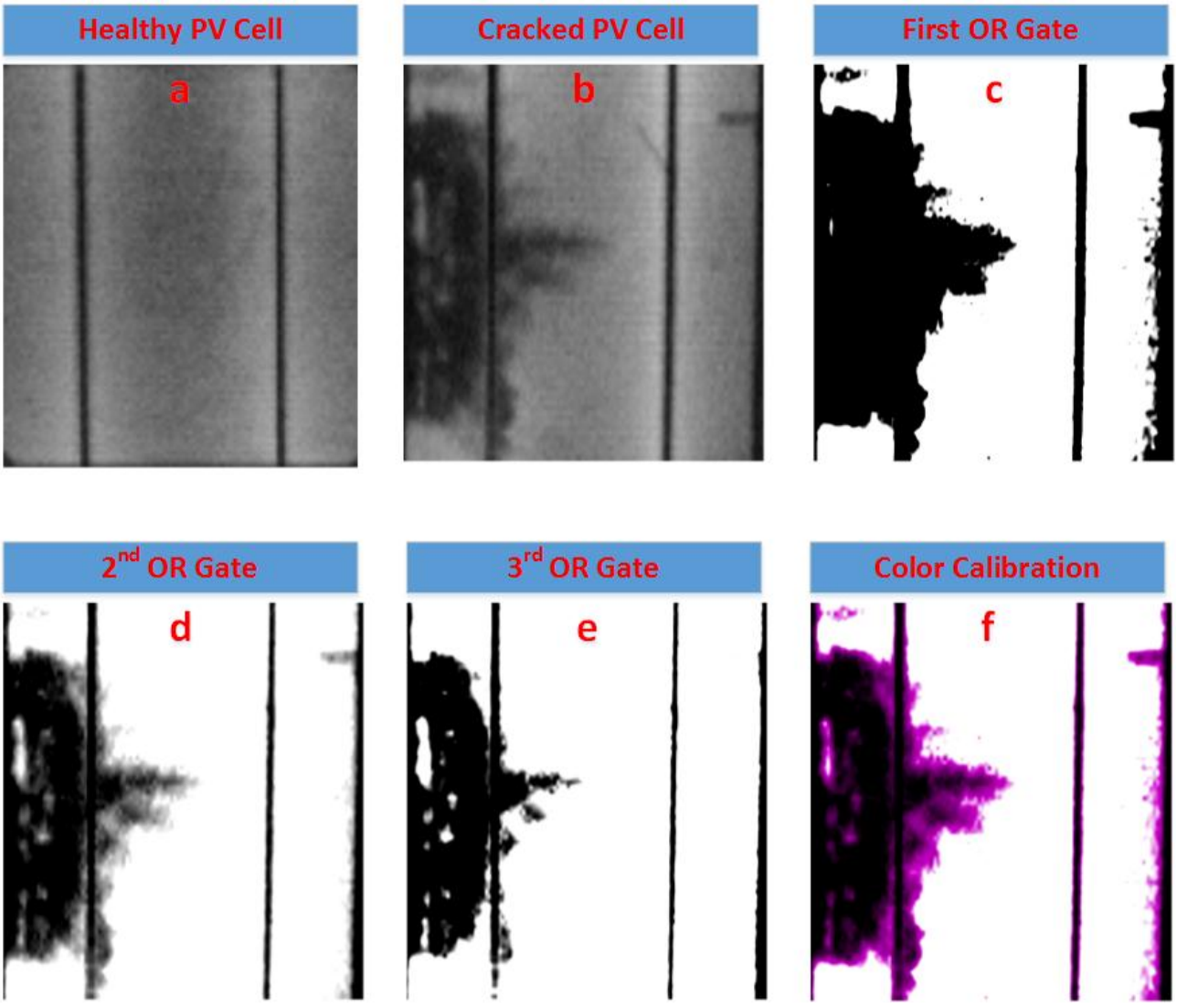

Fig. 7. Output image from the suggesteed 3D graph-based model expalined previosuly in Section 3. (a) Healthy PV cell sample, (b) Cracked PV cell sample, (c) First OR gate output image, (d) Second OR gate output image, (e) Third OR gate output image, (f) Final processed image with color calibration

As stated previously, the final image form the 3rd OR gate will be passed into the color calibration mode as shown in Fig. 7(f). The final output image is modelled using a 3D graph-based technique explained previously in section 4.1. The main purpose of this stage is to examine the loss in the output power of the micro cracked solar cell.

Firstly, the output 3D graph-based model is presented in Fig. 8. The cracked area generates less output power comparing to the free-cracked adjacent area.

The triangle in Fig. 8 shows the area of the PV solar cell which conations micro cracks. This area generates an output power equals to 2.3 W.

However, crack-free (healthy) areas reach a maximum output power of $252 \times 10^{-2} = 2.52$ W (this point is labelled as circle 1 on Fig. 8). Therefore, the maximum loss in the output power due to the crack in the solar cell is equal to equal to:

$$2.52W - 2.3W = 0.22\ W$$

The loss in the output power varies across the tested solar cell sample, since some parts of the solar cell have more micro cracks than the other. Table I reports seven areas compared with the cracked area, these points are labelled on Fig. 8.

The results obtained from Table I shows that the maximum difference between the healthy and cracked peak power is equal to 0.22W (corresponds to 8.7% difference), however, the minimum is obtained at point 5, where the difference equals to 1.3%.

On the other hand, the 3D model gives an optimum layout of the crack and its distribution among the solar cell, thus, it can be used to model, estimate, and observe the impact of the cracks in the solar cell. Further study could use the suggested 3D model to analyse the impact of hot spots in the PV cells, which mostly captured using FLIR cameras [21 – 24].

Table I Comparison between the output power of seven healthy points with the cracked peak power

Point Number	Healthy point Peak power (W)	Healthy point Peak power – cracked peak power (W)	Percentage of the difference in the output power %
1	2.52	2.52 – 2.3 = 0.22	8.7 “maximum”
2	2.48	2.48 – 2.3 = 0.18	7.2
3	2.44	2.44 – 2.3 = 0.14	5.7
4	2.40	2.40 – 2.3 = 0.10	4.1
5	2.33	2.33 – 2.3 = 0.03	1.3 “minimum”
6	2.39	2.39 – 2.3 = 0.09	3.8
7	2.35	2.35 – 2.3 = 0.05	2.1

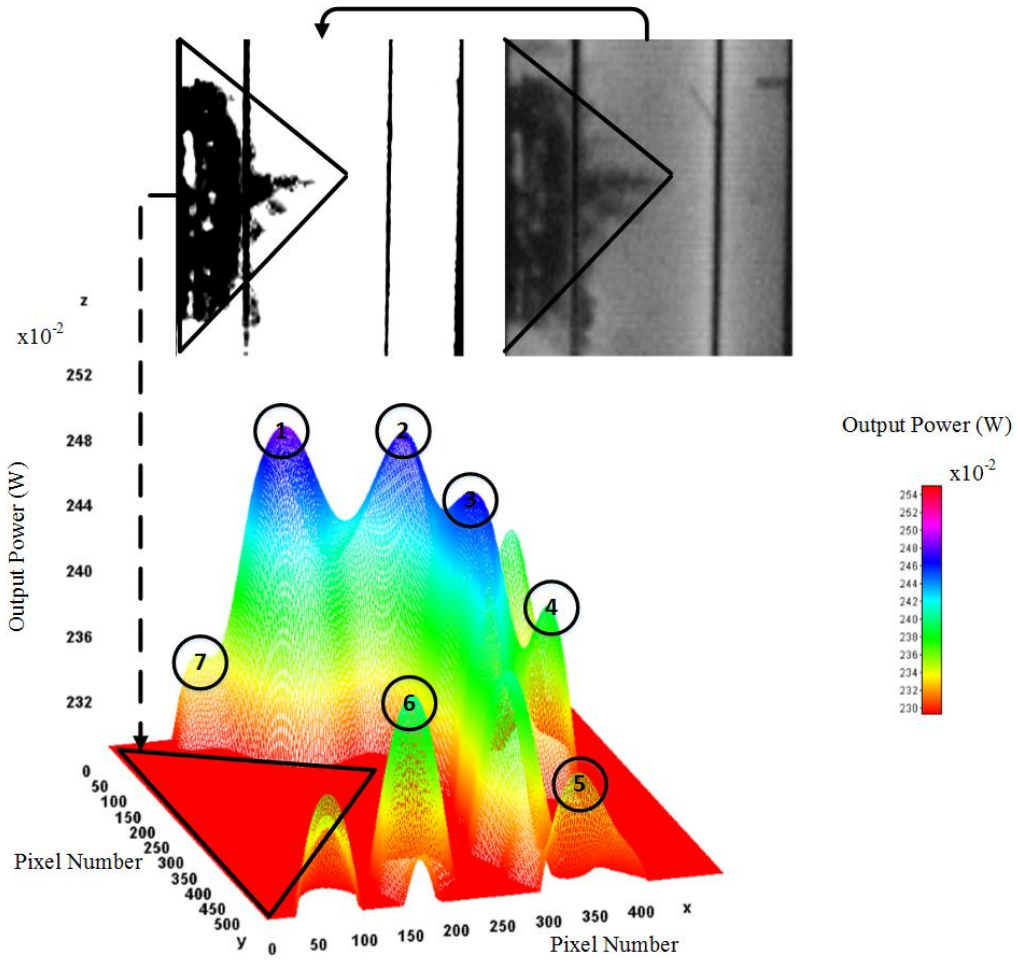

Fig. 8. Output 3D grpah-based model processed using the color calibration image shown in Fig. 7(f)

5. Conclusion

This paper presents a novel technique to examine the impact of Photovoltaic (PV) micro cracks on the output power performance for PV solar cells. Initially, the image of the PV micro crack is captured using Electroluminescence (EL) method, then processed by the proposed technique. The technique consist of two stages as follows:

- First stage: at this stage the combination between a crack-free (healthy) solar cell samples and the cracked solar cell sample will passed into three OR gates. The main functionality of the OR gates is to combine bit-by-bit pixel form both images. Thus reducing the total noise and resulting a high quality calibrated image for the cracked solar cell sample. The final image will then passes into the second stage of the developed technique.

- Second stage: in the second stage, initially a color calibration for the output image from stage one will be accomplished. Next, a 3D surface analysis will be shaped based upon the color calibrated image in order to examine the total loss in the output power caused by the PV micro cracks.

Subsequently, based on the developed 3D graph-based model, this article claims the following:

- PV micro cracks size, location, and orientation are more visible using the proposed technique
- The power loss for cracked solar cells strongly depends on the PV crack size

In future, it is intended to validate the proposed PV micro crack detection and 3D graph-based model in a large scale manufacturing process, where the PV micro cracks often have different sizes, orientation, and locations.

6. Acknowledgment

Authors acknowledge this paper is part of a project collaboration between the Laboratory of Photovoltaics, University of Huddersfield, United Kingdom, and the Electrical Engineering Laboratory (LGE), University MohamedBoudiaf-M'sila, Algeria.

7. References

[1] Y. Liu, B. Li, C. Wu, Y. Zheng, Simulation-based evaluation of surface micro-cracks and fracture toughness in high-speed grinding of silicon carbide ceramics, The International Journal of Advanced Manufacturing Technology. 86 (2016) 799-808. https://doi.org/10.1007/s00170-015-8218-4.

[2] G. C. Eder, Y. Voronko, C. Hirschl, R. Ebner, G. Újvári, W. Mühleisen, Non-Destructive Failure Detection and Visualization of Artificially and Naturally Aged PV Modules, Energies. 11 (2018) 1-14. https://doi.org/10.3390/en11051053.

[3] M. Dhimish, V. Holmes, B. Mehrdadi, M. Dales, P. Mather, PV output power enhancement using two mitigation techniques for hot spots and partially shaded solar cells, Electric Power Systems Research. 158 (2018) 15-25. https://doi.org/10.1016/j.epsr.2018.01.002.

[4] M. Abdelhamid, R. Singh, M. Omar, Review of microcrack detection techniques for silicon solar cells, IEEE Journal of Photovoltaics. 4 (2014) 514-524. https://doi.org/10.1109/JPHOTOV.2013.2285622.

[5] A. Belyaev, O. Polupan, W. Dallas, S. Ostapenko, D. Hess, J. Wohlgemuth, Crack detection and analyses using resonance ultrasonic vibrations in full-size crystalline silicon wafers, Applied Physics Letters. 88 (2006). https://doi.org/10.1063/1.2186393.

[6] W. Dallas, O. Polupan, S. Ostapenko, Resonance ultrasonic vibrations for crack detection in photovoltaic silicon wafers, Measurement Science and Technology. 18 (2007). https://doi.org/10.1088/0957-0233/18/3/038.

[7] Z. Liu, M. Peters, V. Shanmugam, Y. S. Khoo, S. Guo, R. Stangl, A. G. Aberle, J. Wong, Luminescence imaging analysis of light harvesting from inactive areas in crystalline silicon PV modules, Solar Energy Materials and Solar Cells. 144 (2016) 523-531. https://doi.org/10.1016/j.solmat.2015.09.013/.

[8] N. Shiradkar, H. Seigneur, T. R. Newton, S. Danyluk, W. V. Schoenfeld, Effect of laser marks and residual stress in wafers on the propensity for performance loss due to cracking in solar cells, Photovoltaic Specialists Conference (PVSC) 2016 IEEE 43rd. https://doi.org/10.1109/PVSC.2017.8366097.

[9] Y. Zhu, M. K. Juhl, T. Trupke, Z. Hameiri, Photoluminescence imaging of silicon wafers and solar cells with spatially inhomogeneous illumination, IEEE Journal of Photovoltaics. 7 (2017) 1087-1091. https://doi.org/10.1109/JPHOTOV.2017.2690875.

[10] R. Bhoopathy, O. Kunz, M. Juhl, T. Trupke, Z. Hameiri, Outdoor photoluminescence imaging of photovoltaic modules with sunlight excitation. Progress in Photovoltaics: Research and Applications. 25 (2018) 69-73. https://doi.org/10.1002/pip.2946.

[11] M. Dhimish, V. Holmes, M. Dales, P. Mather, M. Sibley, B. Chong, L. Zhang, The impact of cracks on the performance of photovoltaic modules, PowerTech 2017 IEEE Manchester. https://doi.org/10.1109/PTC.2017.7980824.

[12] M. Köntges, M. Siebert, D. Hinken, U. Eitner, K. Bothe, T. Potthof, Quantitative analysis of PV-modules by electroluminescence images for quality control, 24th European Photovoltaic Solar Energy Conference, Germany. (2009) 3226-3232.

[13] T. Fuyuki, A. Kitiyanan, Photographic diagnosis of crystalline silicon solar cells utilizing electroluminescence, Applied Physics A. 96 (2009) 189-196. https://doi.org/10.1007/s00339-008-4986-0.

[14] M. Dhimish, V. Holmes, M. Dales, B. Mehrdadi, Effect of micro cracks on photovoltaic output power: case study based on real time long term data measurements, Micro & Nano Letters. 12 (2017) 803-807. https://doi.org/10.1049/mnl.2017.0205.

[15] M. Kontgers, I. Kunze, S. Kajari-Schroder, X. Breitenmoser, B. Bjorneklett, Quantifying the risk of power loss in PV modules due to micro cracks, 25th European Photovoltaic Solar Energy Conference, Valencia, Spain. (2010) 3745-3752.

[16] S. Kajari-Schröder, I. Kunze, U. Eitner, M. Köntges, Spatial and orientational distribution of cracks in crystalline photovoltaic modules generated by mechanical load tests, Solar Energy Materials and Solar Cells. 95 (2011) 3054-3059. https://doi.org/10.1016/j.solmat.2011.06.032.

[17] S. Oh, D. H. Jun, K. W. Shin, I. Choi, S. H. Jung, J. Choi, W. Park, Y. Park, E. Yoon, Control of Crack Formation for the Fabrication of Crack-Free and Self-Isolated High-Efficiency Gallium Arsenide Photovoltaic Cells on Silicon Substrate, IEEE Journal of Photovoltaics. 6 (2016) 1031-1035. https://doi.org/10.1109/JPHOTOV.2016.2566887.

[18] X. Qian, H. Zhang, C. Yang, Y. Wu, Z. He, Q. E. Wu, H. Zhang, Micro-cracks detection of multicrystalline solar cell surface based on self-learning features and low-rank matrix recovery, Sensor Review. 88 (2018) 360-368. https://doi.org/10.1108/SR-08-2017-0166.

[19] M. Dhimish, V. Holmes, B. Mehrdadi, M. Dales, The impact of cracks on photovoltaic power performance, Journal of Science: Advanced Materials and Devices. 2 (2017) 199-209. https://doi.org/10.1016/j.jsamd.2017.05.005.

[20] C. Solomon, T. Breckon, Fundamentals of Digital Image Processing: A practical approach with examples in Matlab, John Wiley & Sons. (2011).

[21] M. Dhimish, V. Holmes, P. Mather, M. Sibley, Novel hot spot mitigation technique to enhance photovoltaic solar panels output power performance, Solar Energy Materials and Solar Cells. 179 (2018) 72-79. https://doi.org/10.1016/j.solmat.2018.02.019.

[22] I. Geisemeyer, F. Fertig, W. Warta, S. Rein, M. C. Schubert, Prediction of silicon PV module temperature for hot spots and worst case partial shading situations using spatially resolved lock-in thermography, Solar Energy Materials and Solar Cells. 120 (2014) 259-269. https://doi.org/10.1016/j.solmat.2013.09.016.

[23] M. Dhimish, V. Holmes, B. Mehrdadi, M. Dales, P. Mather, Output-power enhancement for hot spotted polycrystalline photovoltaic solar cells, IEEE Transactions on Device and Materials Reliability. 18 (2018) 37-45. https://doi.org/10.1109/TDMR.2017.2780224.

[24] J. Bogenrieder, M. Hüttner, P. Luchscheider, J. Hauch, C. Camus, C. J. Brabec, Technology-specific yield analysis of various photovoltaic module technologies under specific real weather conditions, Progress in Photovoltaics: Research and Applications. 26 (2018) 74-85. https://doi.org/10.1002/pip.2921.